

## MILLIMETER-WAVE IMAGING SENSOR

William J. Wilson, R. J. Howard, Anthony C. Ibbott,  
Gary S. Parks, William B. Ricketts

Jet Propulsion Laboratory  
Pasadena, CA 91109

## Abstract

A scanning 3-mm radiometer system has been built and used on a helicopter to produce moderate resolution ( $0.5^\circ$ ) images of the ground. This mm-wave sensor can be used for a variety of remote sensing applications, and produces images through clouds, smoke, and dust when visual and IR sensors are not usable. The system is described, and imaging results are presented.

## Introduction

A 3-mm radiometer system, with a mechanically scanned antenna, has been built for use on a small aircraft or helicopter to produce near real-time moderate resolution images of the ground. One of the main advantages of this passive imaging sensor is that it is able to provide information through clouds, smoke and dust when visual and IR systems are unusable. This mm-wave imaging sensor can also be used for a variety of remote sensing applications such as measurements of snow cover, surface moisture, vegetation type and extent, mineral type and extent, and surface temperature and thermal inertia. It is also possible to map fires and volcanic lava flows through obscuring clouds and smoke. The fact that the millimeter-wave sensor observes a different physical phenomena, makes it a valuable addition to visual and IR imaging systems.

## System Description

The system configuration is shown in Fig. 1 and the system block diagram is shown in Fig. 2. A lightweight flat reflector is mechanically scanned crosstrack  $\pm 20$  degrees at a 4 Hz rate. A two-axis scanner, controlled by a microcomputer with inputs from both rate and angle gyros, is used to scan the reflector and to correct for aircraft movement due to turbulence. This provides line-of-sight stabilization without the use of a conventional stabilized platform. The two-axis scanner also uses a butterfly scanning pattern to compensate for the forward aircraft motion to produce a linear raster scan pattern on the ground. A  $0.1^\circ$  pointing stability is achieved to eliminate pixel smear and image distortion. The signal from the ground is reflected from the flat scanning mirror onto a 16-inch offset parabolic antenna which focuses the received sig-

nal on the radiometer's feed horn. An offset parabolic antenna was used for its high beam efficiency ( $n_b > 0.9$ ) and low side lobes. Two linearly polarized (H & V) 98 GHz superheterodyne radiometers were used to provide polarization information and to improve the measurement sensitivity. A block diagram of the radiometers is shown in Fig. 3. The radiometers use balanced mixers with beam-lead diodes and one Gunn diode local oscillator is used. The rms noise per ground resolution element is  $< 0.8$  K when both channels are added. A calibrated signal is injected into the feed horn at the end of each scan line to provide temperature calibration. In addition, an ambient load is placed over the feed horn on command to provide additional calibration. The relative accuracy is  $\pm 1$  K and the absolute accuracy is  $\pm 10$  K.

The output signals from the radiometers are digitized, converted to a brightness temperature, and recorded on a digital cartridge tape by a microcomputer. Ground truth data is given by a 35-mm camera and a video camera which record the visual scene. Because the data is taken with stabilized raster pattern, the ground computer system can immediately display the data in false colors on a video monitor. The features which make this system unique from previous airborne mm-wave imaging sensors [1]-[4], are its high resolution, small size, stabilization and computer processing to provide near real-time calibrated images.

## Results

The first test flights of the mm-wave imaging sensor were made in September 1985 with the sensor mounted on a commercial helicopter. All flights were near an altitude of 750 m (2,500 ft) above ground level, and an air speed of  $\sim 90$  km/hr. The objectives of these test flights were to verify the capabilities of this sensor with respect to signal to noise, operation with clouds, and to get mm-wave imaging data on a variety of scenes of cities, highways, farmland, water, and ships. These tests were very successful and samples of the data are shown in Figs. 4 and 5. (Note that the original images, displayed in false colors, are much easier to interpret because of the wider range of colors than the black and white images shown here.)

MM-wave and visual images of an agricultural area west of Fillmore, CA are shown in

Fig. 4. Most of the trees in this area are citrus and there is a dry river bed near the top of the image. All the fields are clearly outlined, and the coldest areas in the fields are standing water and wet soil from irrigation. In the false color images, it is very easy to see where the irrigation water has reached. The small cold areas (~75 K) are storage tanks, vehicles and buildings. The warmest areas are ploughed fields and the dry river bed. In the false color photograph, differences in the mm-wave image of fields were apparent when the visual picture was uniform -- due to differences in the vegetation or soil moisture.

Fig. 5 shows the visual and mm-wave images of the freeway south of Carlsbad, CA on September 26, 1985 during a rainy day. During this day, the mm-wave sensor was flown over a layer of broken clouds which completely obscured the visual images over large areas. On the mm-wave image, the freeways, vehicles, parking lots and buildings are clearly shown as colder targets, reflecting the cooler sky. Vehicles on the freeway, traveling in the same direction as the helicopter, have been stretched while those traveling in the opposite direction were compressed. These vehicles are much easier to "see" on the false color image. This picture clearly shows the ability of the mm-wave imager to provide information on the ground scene when the video image is obscured by the clouds.

A second series of test flights were made in February 1986 near Death Valley, CA to obtain images of desert areas and interesting geological formations. These tests were very successful and examples of this imaging data and a comparison to IR and SAR data will be shown.

### Conclusion

The main thing which is evident from the mm-wave images is that there are many recognizable features at 98 GHz. Also, it is very easy to detect reflective objects such as water, metal objects, highways and buildings because their signals are large compared to the background "clutter". From a study of many images, it is rare that the temperature range is expanded beyond 3 K per color step (which is ~4 times larger than the radiometer noise) since the scene "clutter" is between 2-3 K. It is also interesting, that by properly choosing the range of temperatures, and the order of colors, different features within a scene can "stand out" or "blend in" the picture.

### References

- (1) J.P. Hollinger, J.E. Kenney, and B.E. Troy, Jr., "A Versatile Millimeter-wave Imaging System," IEEE Trans. Microwave Theory Tech., Vol. MTT-24, pp. 786-793, NOV 1976.
- (2) R.P. Moore, "Real-Time Microwave Radiometric Imager," Proc. of Society of Photo-Optical Instrumentation Engineers, Vol. 101, pp. 60-66, APR 1977.

(3) B. Vowinkel, J.K. Peltonen, W. Reinert, K. Grüner and B. Aumiller, "Airborne Imaging System Using a Cryogenic 90 GHz Receiver," IEEE Trans. Microwave Theory Tech., Vol. MTT-29, pp. 535-541, JUN 1981.

(4) J.A. Gagliano and W. Gregorwich, "High-Altitude Atmospheric Measurements at 92/183 GHz Onboard the ER-2 Research Aircraft," in Proc. Eighth Int. Conf. on Infrared and Millimeter-waves, pp. M6.8, DEC 1983.

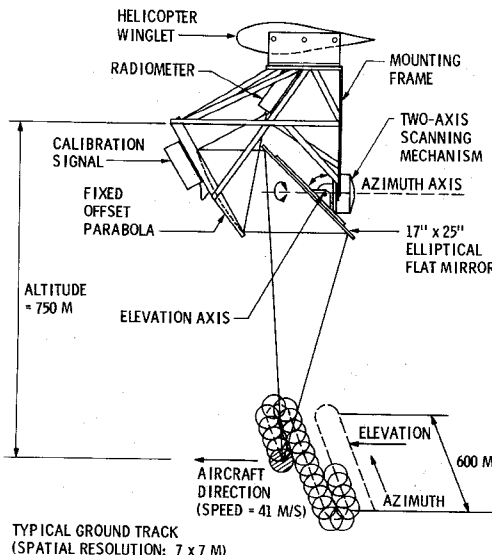


Fig. 1 Configuration of millimeter-wave imaging sensor as flown on the helicopter.

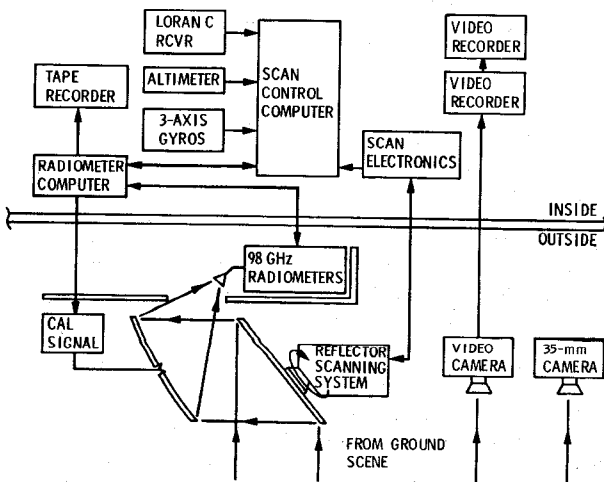


Fig. 2 System block diagram of the millimeter-wave imaging sensor as flown on the helicopter.

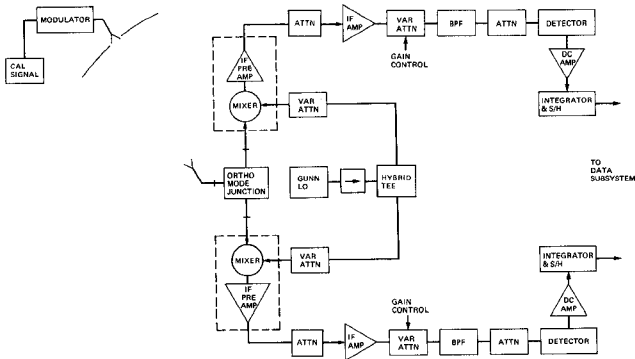


Fig. 3 Block diagram of the dual polarization 98 GHz radiometers and calibration system.

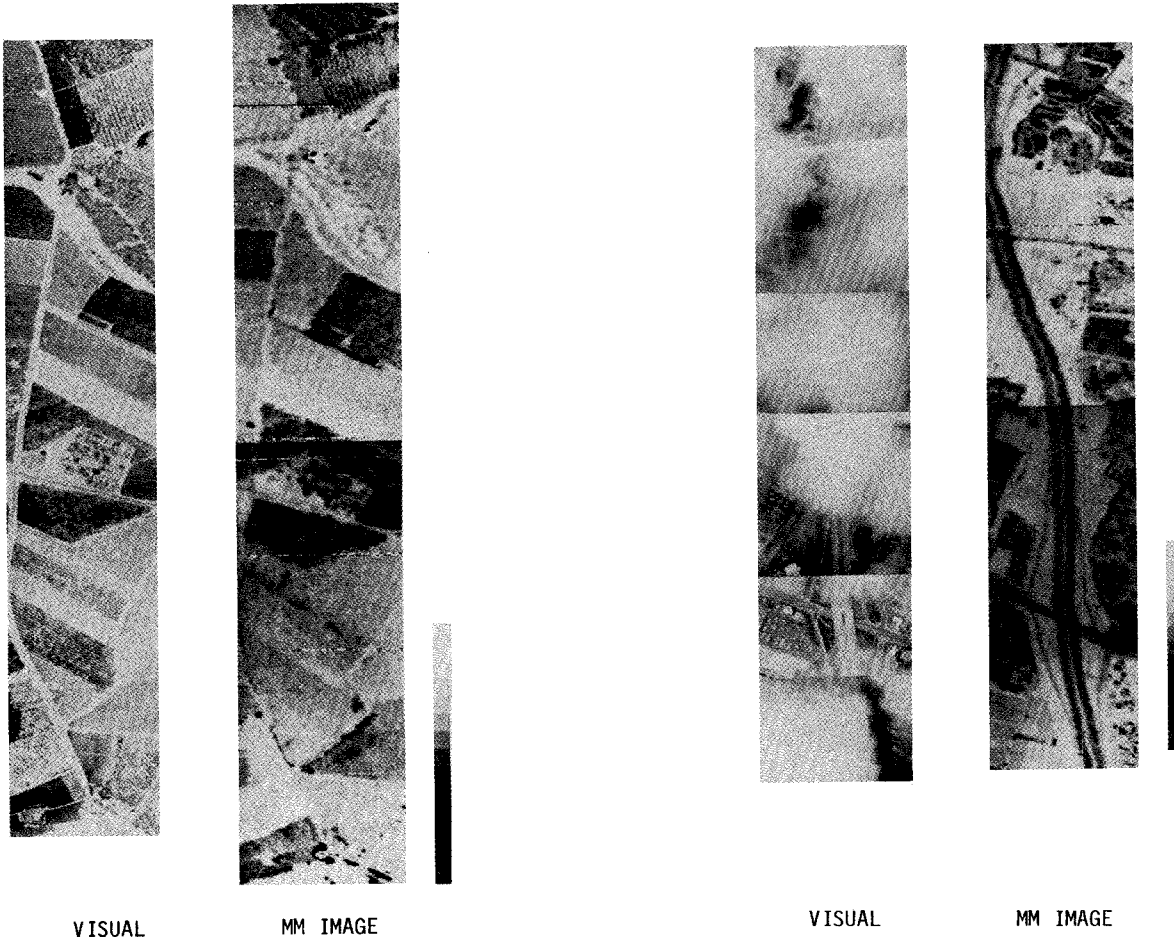


Fig. 4 Video and mm-wave images of a citrus agricultural area west of Fillmore, CA. The cold areas in the fields are water and wet soil from irrigation. The 16-level gray scale is from 250 K (black) to 300 K (white). The scene width is 0.6 km and the length is 2.3 km.

Fig. 5 Video and mm-wave images of a freeway scene, south of Carlsbad, CA on Sept. 26, 1985. During this rainy day, the sensor was flown over a layer of broken clouds as seen in the video pictures. The gray scale is identical to Fig. 4. The scene width is 0.4 km and the length is 1.9 km.